Journal Name

COMMUNICATION

Exquisite Sensitivity of The Ligand Field to Solvation and Donor Polarisability in Coordinatively Saturated Lanthanide Complexes

Kevin Mason[a], Alice C. Harnden[a], Connor W. Patrick[a], Adeline W. J. Poh[a], Andrei S. Batsanov[a], Elizaveta A. Suturina[b], Michele Vonci[c], Eric J. L. McInnes,[c] Nicholas F. Chilton[c] and David Parker*[a]

Crystallographic, emission and NMR studies of a series of C_3-symmetric, nine-coordinate substituted pyridyl triazacyclononane Yb(III) and Eu(III) complexes reveal the impact of local solvation and ligand dipolar polarisability on ligand field strength, leading to dramatic variations in pseudocontact NMR shifts and emission spectral profiles, giving new guidance for responsive NMR and spectral probe design.

The creation of new responsive paramagnetic NMR and emission probes using lanthanide complexes[1,2] relies upon an understanding of the respective factors determining NMR shift and relaxation dynamics and their optical emission spectra, lifetimes and polarisation. In this respect, current proposals that seek to assist creative probe design are restricted in their scope and utility. The importance of the size and sign of the ligand field is implicit in Bleaney's theory of magnetic anisotropy,[3] yet its limitations in chemical shift analysis are increasingly apparent[4] and it can fail palpably in systems with rather small ligand field splittings.[5] Recent work has shown that the size and orientation of the principal component of the magnetic susceptibility tensor determines the pseudo-contact shift,[6,7] in a manner that can be deduced reliably by rigorous magneto-structural correlations.[5]

Similarly, whilst it has been hypothesised that electric susceptibility anisotropy must play a key role in the optical emission analysis of lanthanide(III) complexes,[2] the generally considered static and dynamic aspects of Judd–Ofelt-Mason theory [8,9] fail to offer guiding principles for the design of emission probes. These early theories, however, did highlight the inhomogeneity of local solvation that creates an asymmetric distribution of solvent dipoles around an emissive lanthanide centre, consistent with a key role for solvation in

a) Department of Chemistry, Durham University, South Road, Durham. DH1 3LE, UK
b) School of Chemistry, The University of Southampton, Highfield, Southampton, SO17 1 BJ, UK
c) School of Chemistry, The University of Manchester, Oxford Road, Manchester, M13 9PL, UK

modulating emission intensity .[10] Moreover, it was pointed out that the oscillator strength of 4f-4f transitions is directly related to ligand dipolar polarisabilities and their anisotropies. Thus, variation of the ligand polarisability and its directionality was predicted to be important in the allowed electric quadrupole transitions, that involve induced-dipoles on the ligand and the Ln^{3+} quadrupole moment.[8,9,11]

With this background in mind, we have examined the structure and spectral behaviour of a series of nine-coordinate Eu(III) and Yb(III) complexes [Ln.L$^{1-5}$], in a range of solvents, where the pyridyl ring substituent is varied (Scheme 1). These complexes were prepared by adaptations of literature methods (ESI), and new Yb(III) and Eu(III) complexes were characterised by X-ray crystallography, (Table 1, S1 and Fig S1-2).[12] Crystals were grown by slow-evaporation from water/methanol solutions for all except [Yb.L^4], which was grown by vapour diffusion of diethyl ether into a methanol solution. The [Yb.L^5] complex spontaneously resolved during crystallisation as the Λ enantiomer, (ESI). For each of the other compounds, both enantiomers are present in the unit cell, with the central Ln(III) ion in a slightly distorted tricapped trigonal prismatic coordination, with no coordinated solvent. For [Yb.L^2], [Yb.L^5] and [Eu.L^5] that each crystallised with only water in the lattice, both the carbonyl and the carboxylate oxygen atoms served as hydrogen bond acceptors in a near-linear (~171°) arrangement with the water donor hydrogen atom (Table S1). Hydrogen bonding to the carbonyl oxygen only was observed for [Yb.L^1], [Ln.L^1] (Ln = Nd, Eu, Gd, Tb, Lu)[12] and [Ln.L^3]. [The complex Ln.L^3] crystallises with both water and methanol in the lattice and each solvent participates in hydrogen bonding to carbonyl oxygen atoms. The [Yb.L^4] complex crystallised from MeOH/Et$_2$O, in which a methanol molecule serves as a hydrogen bond donor to the carbonyl oxygen only. No hydrogen bonding involving the *p*-methoxy group was evident in the lattice, consistent with the strong conjugation of the oxygen lone pair into the pyridyl ring. For the Eu and Yb complexes of L^3 (*meta*- ^{t}Bu group), the bond lengths to the carboxylate oxygen were about 0.05 Å shorter, and the Ln-N$_{py}$ distances about 0.1 Å longer, giving rise to a
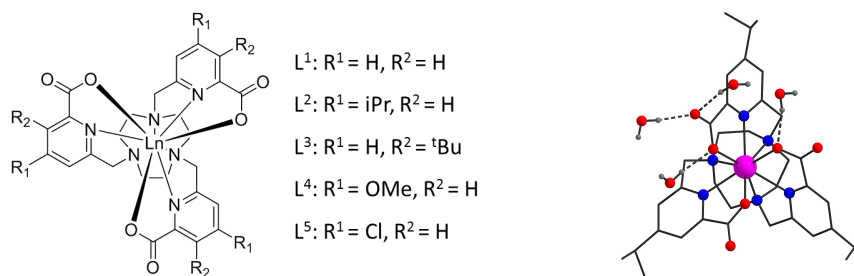
Scheme 1 Left: Molecular structure of [Ln.L$^{1-5}$] (Ln=Eu(III) or Yb(III)) complexes. Right: X-ray crystal structure of [Yb.L^2] with partial H-bonding displayed, for full H-bonding see Figure S1.

significantly different ligand field, presumably caused by the steric demand of the ^{t}Bu substituent.

We recently showed for [Ln.L^1] (Ln = Eu-Yb), how the second-order crystal field coefficient, usually written as B_0^2, can be very sensitive to minor structural variations induced by the choice of solvent, and that these perturbations are not constant across the later Ln series.[5] Indeed, we showed that changes in the magnitude and sign of the axiality of the magnetic susceptibility tensor explains the solvent dependence of the paramagnetic shift in [Ln.L^1]. The choice of solvent influences the average polar angle of the oxygen donor atoms, that become slightly more 'axial', (< 2°) as H-bonding ability and solvent polarity increase. Our initial study was limited to water, methanol and DMSO because of solubility constraints.[5a] The structural work reported here strongly supports our hypothesis, suggests that H-bonding to the coordinated carboxylate oxygen atoms 'tugs' at these O$_3$ donors, causing a change in the spectroscopic mean B_0^2 value.

The ^{1}H NMR spectra of the isopropyl-substituted analogue, [Yb.L^2], were examined, as this complex is soluble in a wider range of solvents, (Figure 1). The observed pseudocontact shift correlates rather well (Fig S4, R^2 = 0.93) with Reichardt's empirical solvent polarity parameter, E$_T$-30, [13] and the very large shift changes suggest that this complex can be considered as an NMR solvent polarity probe. The behaviour of the m-^{t}Bu-substituted complex [Yb.L^3] is rather different and much smaller pseudo-contact shifts are observed, compared to [Yb.L^2] (Fig S5), consistent with the changes in the Ln-N and

Ln-O bond lengths and a smaller ligand field (Tables 1 and S2). For each of the Yb complexes examined, the sign of B_0^2 also changes, going from D$_2$O to CD$_3$OD.[5a] Based on earlier work examining relaxation rate sensitivity to ligand substitution,[5b] the magnitude of B_0^2 was hypothesised to be a sensitive function of the electrostatic interaction between the Ln^{3+} ion and the pyridyl group. The strength of this bonding interaction is modulated by variation of the p-substituent in the pyridine ring. Proton NMR spectra for [Yb.L^{1,2}] and [Yb.L^{4,5}] highlight the sensitivity of the electronic structure to this perturbation (Figure 2). Comparing the assigned spectra in CD$_3$OD and D$_2$O, it is evident that the paramagnetic shift sequence is *opposite*, being largest in D$_2$O for the p-Cl derivative, [Yb.L^5] (compare pro-R and ring H$_{ax}$ resonances) and largest in CD$_3$OD for the p-OMe derivative, [Yb.L^4]. The pseudocontact shift of a given resonance, or simply the total spectral width, correlates well with the Hammett σ_p parameter in D$_2$O and CD$_3$OD (R^2 = 0.93, 0.97 respectively, Fig S6), consistent with the strongly dipolar nature of the Ln^{3+}/N$_{py}$ bond.

Our recent work has shown the sensitivity of the electronic structure to the polar angle of the oxygen donor atoms, θ,[5a] representing the angle subtended by the average Ln-O vector with respect to the molecular C$_3$ axis. As θ lies close to the 'magic' angle for these complexes, small changes can cause a major change in the magnetic susceptibility anisotropy.[14] We have employed DFT calculations to determine a pseudo-solution structure in H$_2$O with imposed C$_3$ symmetry as described previously,[5a] and then used CASSCF-SO calculations to extract the anisotropy of the susceptibility tensor, (squares, Figure 3). Because changes to the structural part of Equation 1

Table 1 Selected average bond lengths (Å) and average angles for [Ln.L$^{1-5}$] in the crystalline phase. [a]

Complex	θ	Ln-N	Ln-N$_{py}$	Ln-O
[Yb.L^1]	50.0	2.605	2.483	2.306
[Yb.L^2]	50.1	2.603	2.466	2.327
[Yb.L^3]	51.3	2.605	2.568	2.273
[Yb.L^4]	50.3	2.617	2.468	3.323
[Yb.L^5]	50.3	2.600	2.491	2.310
[Eu.L^1][b]	51.4	2.673	2.556	2.390
[Eu.L^3]	52.1	2.653	2.621	2.347
[Eu.L^5]	50.9	2.696	2.550	2.386

[a] θ represents the average angle subtended by the molecular pseudo-C$_3$ axis with the Ln-O vector; [b] data from reference 12. CCDC: 1849021-1849027 and 1850294.
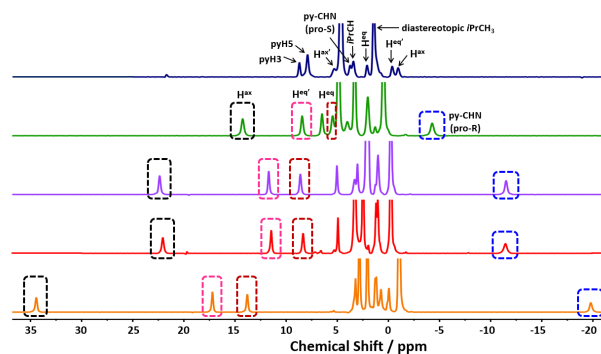

Figure 1 ^{1}H NMR spectra of [Yb.L^2] in D$_2$O (blue), CD$_3$OD (green), CD$_3$CN (purple), DMSO-d$_6$ (red) and acetone-d$_6$ (orange), (200 MHz, 295 K). Proton labelling scheme, Fig S3.
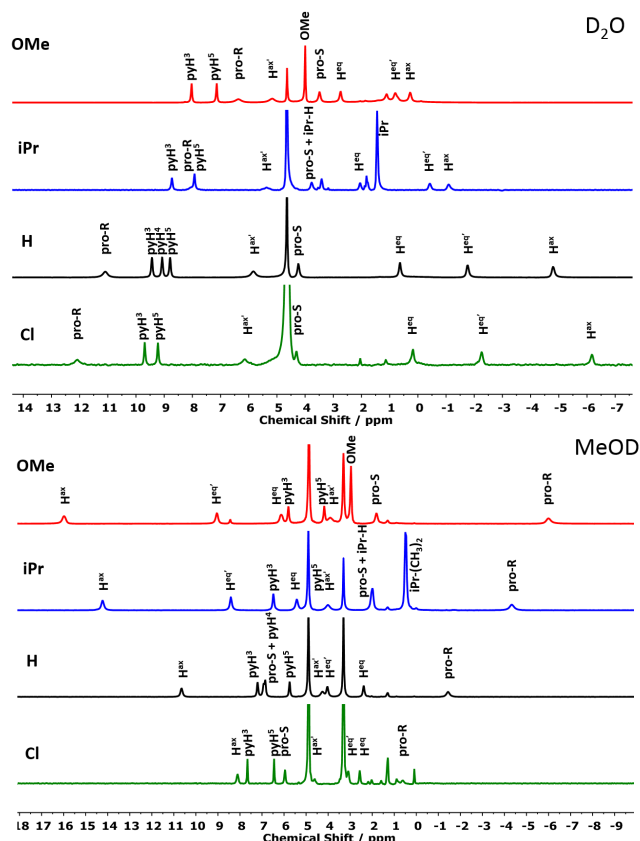
Figure 2 Proton NMR spectra of the pyridyl complexes with the shown *p*-substituent, in D$_2$O (upper) and CD$_3$OD (lower), (295 K, 4.7 T) showing inverse shift behaviour. The proton labelling scheme is given in Fig S3.

$$\delta_{pc} = \frac{\chi_{\parallel} - \chi_{av}}{2N_A}\left(\frac{3\cos^2\theta - 1}{r^3}\right) \qquad (1)$$

(N$_A$ is Avogadro's number, $\chi_{\parallel} - \chi_{av}$ is the anisotropy of the molar magnetic susceptibility in cm^3 mol^{-1}, and θ, r are the polar coordinates of the ^{1}H nucleus with respect to the principal axis of the magnetic susceptibility tensor) for small changes in θ are negligible,[5a] we are able to determine the experimental values of $\chi_{\parallel} - \chi_{av}$ assuming a fixed structural model using the experimental pseudocontact shifts referenced to the chemical shifts of the diamagnetic Y complexes. Using the experimental values in five solvents (D$_2$O, CD$_3$CD, CD$_3$CN, d$_6$-DMSO and d$_6$-acetone, for calculations see Figure S8), we compare these to our CASSCF-SO-calculated susceptibility anisotropy to determine the spectroscopic average value of θ in solution.

Inspection of Figure 3, clearly shows that [Yb.L^2] can be considered as an NMR probe of solvent polarity owing to the sensitive variation of susceptibility anisotropy with θ (covering 2.8°). Indeed, the susceptibility anisotropy (and therefore pseudocontact shift) changes sign in D$_2$O, the most polar solvent examined here in which the strongest H-bonding interactions to both carboxylate oxygen atoms was observed in the solid-state (Table S1). The chemical shift non-equivalence of the methyl groups in the ^{i}Pr substituent, Δδ$_{Me}$, also increases in proportion to solvent polarity (Fig S7),
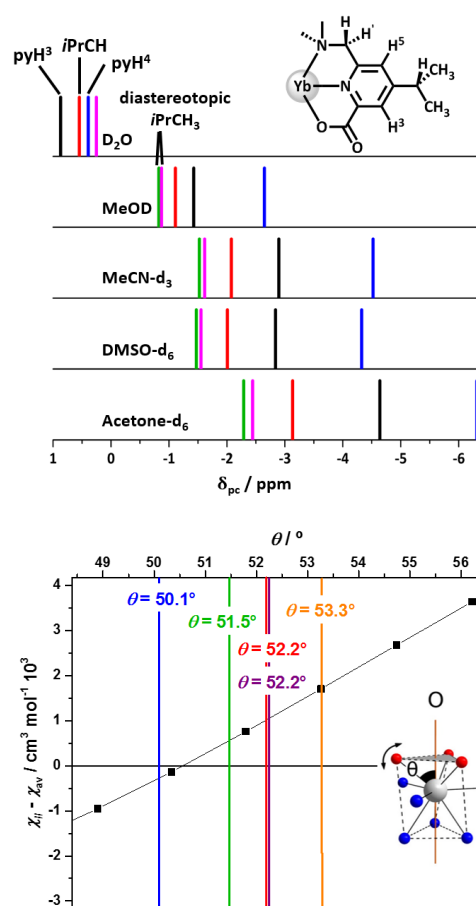

Figure 3 Schematic representation of the pseudocontact shifts (295 K, 4.7 T) for pyridine H^3, H^5 and isopropyl resonances for [Yb.L^2], calculated from the diamagnetic shifts of [Y.L^2] and the variation in the susceptibility anisotropy with the polar angle θ, in the stated solvents D$_2$O (blue); CD$_3$OD (green); CD$_3$CN (purple), DMSO-d$_6$ (red) and acetone-d$_6$ (orange); the diastereotopic methyl resonances are isochronous in D$_2$O only.

offering a direct NMR means of assessing polarity, without the need to evaluate δ$_{pc}$ by subtraction of shift data for the analogous diamagnetic [Y.L^2] complex. The largest shift non-
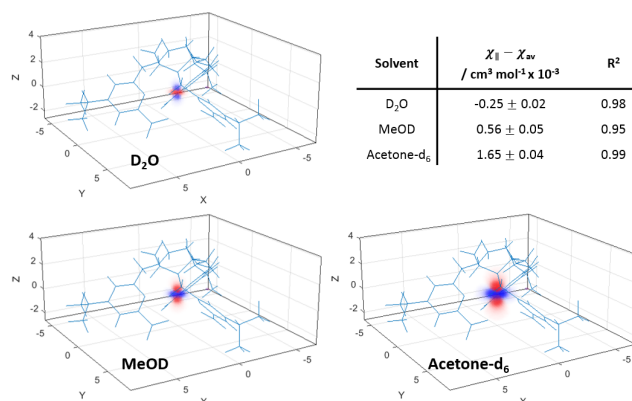

Solvent	$\chi_{\parallel} - \chi_{av}$ / cm^3 mol^{-1} x 10^{-3}	R^2
D$_2$O	-0.25 ± 0.02	0.98
MeOD	0.56 ± 0.05	0.95
Acetone-d$_6$	1.65 ± 0.04	0.99

Figure 4 The pseudocontact shift fields for [Yb.L^2], (calculated using Spinach)[15], in the stated solvents showing positive PCS in red and negative in blue. The Table shows the calculated anisotropy of the magnetic susceptibility extracted from a linear fitting of the structural part of eq. 1 to the experimental PCS data (Fig. S8).

equivalence is observed in d_6-acetone, and pseudo-contact shift fields in acetone, water and methanol were computed using Spinach [15] (Fig. 4), highlighting this sensitivity to solvent change. In D_2O, the PCS field shows the pronounced change in sign as the magnetic susceptibility anisotropy switches from 'easy axis' in other solvents to 'easy plane' in D_2O.

Emission spectra for [Eu.L$^{1-5}$] were recorded in at least six solvents, and the spectral form revealed a marked dependence on the nature and polarity of the solvent (Figs S9 and S10), as well as a variation with the nature of the pyridyl substituent. In the latter case, a linear plot of (derived from the splitting of the major/minor $\Delta J = 1$ transition components in the spherical tensor notation [14]) versus σ_p was obtained in CD_3CN (Fig S11, $R^2 = 0.97$). The variation with solvent for a given complex led to comparable changes across the series, illustrated by the behaviour of [Eu.L^4], which was sufficiently soluble to be studied in 12 different solvents, Figure 5.

We found a weak correlation between B_0^2 and E_T–30 (Fig S13). In $CHCl_3$ the $\Delta J = 0$ transition gained intensity (J mixing), and the $\Delta J = 1$ splitting was as small as in water, suggesting rather different behaviour. Indeed, direct evidence for complex aggregation was found by DOSY NMR analysis of the Y(III) analogue; this aspect will be reported separately. The hypersensitive $\Delta J = 2$ and $\Delta J = 4$ manifolds also varied markedly as a function of solvent and the relative intensity of pairs of bands, in each case, showed weak positive correlations with polarity for adjacent pairs in the $\Delta J = 2$ manifold (Fig S12).

In summary, these detailed NMR and emission spectral analyses highlight the exquisite sensitivity of the ligand field to the nature of the solvent, primarily arising from medium polarity effects. In water and polar, protic media, evidence for specific solvent interactions was found, ascribed to hydrogen bonding to the ligand carboxylate oxygen atoms. In addition, the well defined solvent polarity effects on pseudocontact shift can be attributed to the orientation of solvent dipoles that perturb the Ln-O and Ln-N$_{py}$ dipolar and quadrupolar interactions, as anticipated by earlier theoretical work.[8,9,11] The com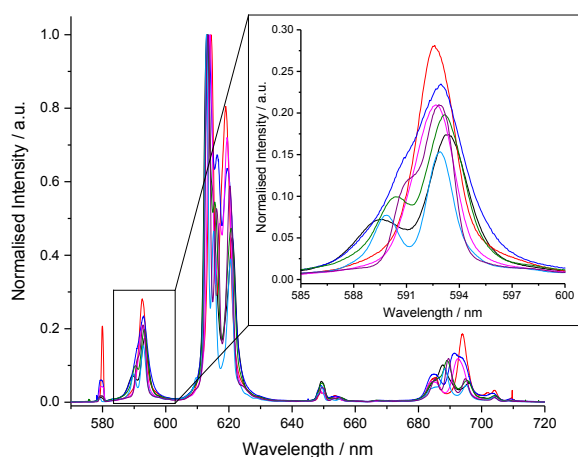plex, [Yb.L^2] can be considered as the first paramagnetic shift probe of solvent polarity, using the shift separation of the diastereotopic isopropyl methyl groups as the observable parameter, as verified by our magneto-structural correlation. Moreover, the sensitivity of the shift and emission profiles of these complexes to the nature of the pyridine *para*-substituent emphasises the importance of overall dipolar polarisability in determining ligand field.

Conflicts of interest

There are no conflicts to declare.

References

1   M.C.Heffern, L.M. Matosziuk, T.J. Meade, *Chem. Rev.*, 2014, 114, 4496

2   O.A. Blackburn, R.M. Edkins, S. Faulkner, A.M. Kenwright, D. Parker, N.J. Rogers and S. Shuvaev, *Dalton Trans*. 2016, 45, 6782

3   B. Bleaney, *J Magn. Reson*. 1972, 8, 91; C. Piguet, C.F.G.C. Geraldes, 'Paramagnetic NMR Lanthanide Induced Shifts for Extracting Solution Structures' in 'Handbook on the Physics and Chemistry of Rare Earths', Elsevier, 2003, Vol. 33, pp 353-463

4   A.M. Funk, K.N.A. Finney, P. Harvey, A.M. Kenwright , E.R. Neil , N.J. Rogers, P.K Senanayake and D. Parker, *Chem. Sci.*, 2015, 6, 1655; G. Castro, M. Regueiro-Figueroa, D. Esteban-Gómez, P. Pérez-Lourido, C. Platas-Iglesias, and L. Valencia, *Inorg. Chem.*, 2016, 55, 3490

5   a) M. Vonci, K. Mason, E.A. Suturina, A.T. Frawley, S.G. Worswick, I. Kuprov, D. Parker, E.J.L. McInnes, and N.F. Chilton, *J. Am. Chem. Soc.*, 2017, 139, 14166; b) N. J Rogers, K-L N. A. Finney, P. K. Senanayake and D. Parker, *Phys. Chem. Chem. Phys.* 2016, 18, 4370-4375.

6   O.A. Blackburn, N.F. Chilton, K Keller, C.E. Tait, W.K. Myers, E.J.L. McInnes, A M. Kenwright, P.D. Beer, C.R. Timmel, S. Faulkner, *Angew. Chem. Int. Ed*., 2015, 54, 10783

7   E.A. Suturina, K. Mason, C.F.G.C. Geraldes, I. Kuprov, D Parker, *Angew. Chem. Int. Ed*., 217, 40, 12215

8   S.F. Mason, R.D. Peacock & B. Stewart, *Mol. Phys.*, 1975, 30, 1829; S.F. Mason, *Struct. Bonding*, 1980, 39, 43.

9   M.F. Reid, F.S. Richardson, *Chem. Phys. Lett*. 1983, 95, 5012

10 G.S. Ofelt, J. Chem. Phys., 1962, 37, 511; B.R. Judd, *Phys. Rev.*, 1962, 127, 750; C.K. Jorgensen and B.R. Judd, *Mol. Phys.*, 1964, 8, 281

11 R. Kuroda, S.F. Mason and C. Rosini, *J. Chem. Soc., Faraday Trans. 2*, 1981, 77, 2125; F.S. Richardson, *Chem. Phys. Lett.,* 1982, 86, 47

12 For [Tb.L^1] see: G. Nocton, A. Nonat, C. Gateau and M. Mazzanti, *Helv. Chim. Acta*, 2009, 92, 2257; for Nd, Eu, Gd and Lu analogues see: C. Gateau, M. Mazzanti, J. Pécaut, F.A. Dunand and L. Helm, *Dalton Trans.*, 2003, 2428-2433.

13 a) C. Reichardt, T. Welton, 'Solvents and Solvent Effects in Organic Chemistry'; b) C. Reichardt, T. Welton eds., Wiley-VCH, Weinheim, Germany, 2010, pp 425-508.

14. C. Gorller-Walrand, E. Huygen, K. Binnemans, L. Fluyt, *J. Phys. Condens. Matter* 1994, 7797.

15. H. J. Hogben, M. Krzystyniak, G. T. P. Charnock, P. J. Hore, I. Kuprov, *J. Magn. Reson*. 2011, 208, 179.

Figure 5 The emission spectrum of [Eu.L^4] in CH_2Cl_2 (black), $CHCl_3$ (red), CCl_4 (blue), D_2O (magenta), THF (green), 1,4-dioxane (purple) and DMSO (light blue) (298 K, λ_{exc} = 268 nm). Spectra are normalised to the highest intensity transition; an expansion of the $\Delta J = 1$ manifold is shown that allows estimation of the ligand field parameter, B_0^2.